symmetry

MDPI

Article

Symmetries of the Electromagnetic Turbulence in a Tokamak Edge

Giovanni Montani [1,2] and Fabio Moretti [1,*]

[1] Fusion and Nuclear Safety Department, ENEA, C. R. Frascati, Via E. Fermi 45, 00044 Frascati, Italy; giovanni.montani@enea.it
[2] Physics Department, "Sapienza" University of Rome, P.le Aldo Moro 5, 00185 Roma, Italy
* Correspondence: fabio.moretti.1@enea.it

Abstract: We construct the low-frequency formulation of the turbulence characterizing the plasma in a Tokamak edge. Under rather natural assumptions, we demonstrate that, even in the presence of poloidal magnetic fluctuations, it is possible to deal with a reduced model for turbulence dynamics. This model relies on a single equation for the electric potential from which all the physical turbulent properties can be calculated. The main result of the present analysis concerns the existence of a specific Fourier branch for the dynamics which demonstrate the attractive character of the two-dimensional turbulence with respect to non-axisymmetric fluctuations. The peculiar nature of this instability, affecting the non-axially symmetric modes, is discussed in some detail by recovering two different physical regimes.

Keywords: non-linear fluid dynamics; axisymmetric modes; plasma turbulence; Tokamak edge physics

1. Introduction

One of the most important phenomena affecting the transport processes in a Tokamak edge is the turbulence affecting the plasma in that region [1–4]. This turbulent behavior is due to a number of different physical ingredients [5–7], but one of the most relevant contributions is certainly due to the so-called non-linear drift response, as discussed in [8]; see also the review in reference [9]. The drift turbulence is a non-linear self-sustained process, which receives a linear triggering in terms of the free energy available to the spectrum development from the background pressure gradient [10–13]. However, the non-linear dynamics of the system are then independent of this linear triggering, even because this source of linear instability is significantly suppressed in the presence of magnetic shear [8].

The theoretical ground of the non-linear drift response is a two-fluid model (electrons and ions), which is justified by the plasma conditions (the low density and the temperature) of the edge plasma and the assumption of low-frequency physics, in which the typical time scale of the turbulent processes is long in comparison to the inverse of the ion gyrofrequency. The original Hasegawa–Wakatani formulation describing the drift turbulence dynamics in [10,11] has been based on the effective representation of the Fourier evolution, de facto reducing the problem to a two-dimensional picture [14–17]. The limits of this representation and the impact of dealing with a realistic three-dimensional scenario have been discussed in [18] (for a recent systematic analysis on this aspect, see [19]).

However, we remark that despite the fact that the simple electrostatic formulation of the turbulence captures many real features of the non-linear dynamics in currently operating systems, nonetheless, as the plasma β-parameter increases enough, a poloidal fluctuation of the magnetic field becomes a relevant subject of the turbulent behavior [8].

In a recent study [20], see also [21], an electrostatic reduced model has been proposed, which leads to a single equation for the electrostatic potential field, as a result of neglecting the linear instability trigger and taking a unique coefficient to describe both the shear viscosity and the particle diffusion; see [18]. As an important issue, this reduced model was

check for updates

Citation: Montani, G.; Moretti, F. Symmetries of the Electromagnetic Turbulence in a Tokamak Edge. *Symmetry* **2024**, *16*, 1111. https://doi.org/10.3390/sym16091111

Academic Editors: Tomohiro Inagaki and Fabio Sattin

Received: 8 July 2024
Revised: 20 August 2024
Accepted: 22 August 2024
Published: 26 August 2024

Copyright: © 2024 by the authors. Licensee MDPI, Basel, Switzerland. This article is an open access article distributed under the terms and conditions of the Creative Commons Attribution (CC BY) license (https://creativecommons.org/licenses/by/4.0/).

able to predict the attractive character of the two-dimensional axisymmetric configuration with respect to the parallel fluctuations. Since the magnetic field has been taken to be constant and uniform along the axial direction, the obtained picture can be qualitatively associated to the spectral features of the plasma close enough to the X-Point of the magnetic configuration of a Tokamak device.

Here, starting with a rather general picture of the low-frequency turbulence, we then implement a number of motivated simplifications which again lead to a reduced model, characterized by a single equation for the electric field potential. The main difference of the present model with respect to previous ones, having the same scheme, is that here we include the axial potential vector amid fluctuations, which is found to be responsible for a turbulent poloidal magnetic field. Like in previous studies [20,22], a constitutive relation links the number density fluctuation to the vorticity field. Moreover, we show that it is possible to evaluate the axial vector potential from the electric field, via one of the basic dynamical equations.

We provide an analytical study, showing the attractivity of the two-dimensional axisymmetric spectrum also in the presence of a turbulent poloidal magnetic field. In fact, we determine a decaying branch of the non-axially symmetric perturbation, as an exact solution of the considered dynamics in the Fourier space. We observe that the obtained decaying behavior has two different characteristic regions of the dispersion relation, associated to a non-zero and zero real frequency, respectively. These two decaying regimes both differ from the corresponding spectral behavior of the pure electrostatic case and, overall, they are not directly connected to the value of the toroidal wave number n: below a given n-dependent wave number, the decaying rate is not affected at all by n itself, while a dependence emerges in the toroidal spectral region above this value (additionally, the dependence is different from the electrostatic case).

This result offers an interesting scenario also for incoming large-size Tokamak machines, like the Italian DTT [23,24] or the ITER. In fact, we can conclude that, close enough to the X-point configuration, the turbulence has mainly a two-dimensional spectral feature even when the β-parameter of the plasma is considerably large with respect to the currently operating Tokamak [5,6]. We conclude this introduction by discussing some of the approximations underlying our analysis. First of all, we consider a two-fluid low-frequency model to describe the electromagnetic edge turbulence. This approach is reliable in many physical contexts for the Tokamak edge turbulence, since the typical space and time scales of the edge turbulence are typically larger than the ion Larmor radius and the gyro-time, respectively. Clearly, in future fusion devices like the ITER, scenarios can be explored in which gyro-fluid and gyro-kinetic corrections to the turbulence dynamics can be significant [9]. However, the major impact on the outward heat and particle transport is expected to be driven by the low-frequency non-linear drift response, which is surely one of the basic ingredients to account for the so-called anomalous transport [1]. Furthermore, we arrive to formulate a reduced model for the electromagnetic turbulence, based on the possibility to neglect the background pressure gradients and the ion axial velocity. Despite this restriction, our non-linear dynamics are able to capture the basic features of the turbulence profile. In fact, as discussed in [9], it is clearly stated how the intrinsic feature of the edge turbulence is due to the self-sustained (i.e., not supported by the background free energy) non-linear drift response. In other words, in a fully developed turbulence scenario, the presence of the background pressure gradients has a very limited impact on the non-linear fluctuation evolution (for a validation of this statement in the case of the electrostatic turbulence, see [19]). In this regime, the main source of the turbulence profile is, on the one hand, in the non-linear self-interaction of the electric field, and on the other hand, in the advection of the perturbed pressure and the coupling of both the pressure and the electric field to the axial vector potential [8]. Also, the toroidal ion velocity can be a regarded as a negligible effect, except for those configurations in which either the external beam injection or a phenomenon of spontaneous rotation are considered. These

two effects concern the specific operational conditions of a Tokamak and they should be treated separately with respect to the standard turbulence dynamics we address here.

The manuscript is organized as follows: in Section 2, we present the hypotheses on which our model of electromagnetic edge turbulence is grounded, deriving the basic dynamical equations and formulating the problem in adimensional variables. In Section 3, we recast the set of PDE obtained in order to highlight the fact that they represent a generalized version of the Hasegawa–Wakatani model. In Section 4, we make further assumptions, well-justified in the case of a Tokamak plasma scenario, showing how the system of PDE results is condensed in a single governing equation for the electric potential. Fourier analysis is then performed on this unique equation, outlining the presence of two distinct branches of the dispersion relation. Conclusions are finally drawn in Section 5.

2. Construction of the Model

We analyze the dynamical and physical properties of the plasma laying in the edge region of a Tokamak machine with particular reference to the magnetic X-point zone, placed out of the separatrix. We consider a quasi-neutral hydrogen-like plasma, in the low-frequency limit (i.e., the phenomenon evolution rates are much smaller than the ion gyrofrequency Ω_i), and we provide a two-fluid representation of its dynamics, within the so-called "drift ordering approximation".

The equilibrium magnetic configuration is here modeled via a constant and uniform magnetic filed. Choosing a set of Cartesian coordinates $\{x, y, z\}$ (the relative versors are denoted by $\mathbf{e}_x$, $\mathbf{e}_y$ and $\mathbf{e}_z$, respectively), the background magnetic field is expressed as $\mathbf{B} = B_0\mathbf{e}_z$, with $B_0 = const.$ (henceforth, the suffix 0 will denote background quantities). The z-axis must be thought of as the toroidal axis of a Tokamak device. It is worth noting how the use of Cartesian coordinates still offers a suitable representation of the addressed physical context. In fact, the z coordinate is here associated with a closed topology, well-reproducing the toroidal profile of a Tokamak device. As implicitly assumed here, the magnetic field curvature is a higher order effect in the turbulent dynamics [8,10,11]. The x-y coordinates well describe the poloidal plane since, assuming a purely toroidal magnetic field, we intend our formulation to be well appropriate to the vicinity of a Tokamak X-point only.

In the proposed approximation scheme, and neglecting diamagnetic effects, the electron momentum balance provides for the orthogonal electron velocity $\mathbf{v}_\perp$ in the following $\mathbf{E} \times \mathbf{B}$ expression:

$$\mathbf{v}_\perp \equiv \mathbf{v}_E = \frac{c}{B_0}\left(-\partial_y\phi\mathbf{e}_x + \partial_x\phi\mathbf{e}_y\right), \tag{1}$$

where $\phi(t, x, y, z)$ denotes the electric potential fluctuation (here, we neglect any background contribution). In what follows, the advective (Lagrangian) derivative is constructed with $\mathbf{v}_E$, namely

$$\frac{df}{dt} \equiv \partial_t f + \frac{c}{B_0}\left(\partial_x\phi\partial_y f - \partial_y\phi\partial_x f\right), \tag{2}$$

in which f is a generic scalar or vector function. The ion momentum balance provides the dynamical equation for the ion perpendicular velocity $\mathbf{u}_\perp$

$$\frac{d\mathbf{u}_\perp}{dt} = \frac{e}{M_i}\left(-\boldsymbol{\nabla}_\perp\phi + \frac{\mathbf{u}_\perp}{c} \times \mathbf{e}_z B_0\right) + \nu\Delta_\perp\mathbf{u}_\perp, \tag{3}$$

where e is the elementary charge, M_i the ion mass and ν denotes the constant kinematic (perpendicular) ion viscosity.

If, in agreement with the low-frequency approximation, we set $\mathbf{u}_\perp = \mathbf{v}_E + \mathbf{u}_\perp^{(1)}$, where the correction to the $\mathbf{E} \times \mathbf{B}$ velocity is taken to be small, then Equation (3) gives, at a first order,

$$\mathbf{u}_\perp^{(1)} = \mathbf{e}_z \times \frac{1}{\Omega_i}\left(\frac{d\mathbf{v}_E}{dt} - \nu\Delta_\perp\mathbf{v}_E\right), \tag{4}$$

in which the first term in parenthesis corresponds to the so-called polarization drift velocity. We see how, according to the low-frequency approximation adopted for the dynamics, the polarization drift velocity is a small correction to the $\mathbf{E} \times \mathbf{B}$ velocity, just because the typical turbulence frequency is much smaller than Ω_i.

The charge conservation equation $\boldsymbol{\nabla}_\perp \cdot \mathbf{j}_\perp = -\boldsymbol{\nabla}_\parallel \cdot \mathbf{j}_\parallel$ can be easily restated by observing that $\mathbf{j}_\perp = n_0 e \mathbf{u}_\perp^{(1)}$, where we indicate with n_0 the electron and ion background density. Hence, we get the following equation:

$$\partial_t \Delta_\perp \phi + \frac{c}{B_0}\left(\partial_x \phi \partial_y \Delta_\perp \phi - \partial_y \phi \partial_x \Delta_\perp \phi\right) = 4\pi \frac{v_A^2}{c^2} \partial_z j_z + \nu \Delta_\perp^2 \phi \,, \tag{5}$$

where $v_A = B_0/\sqrt{4\pi n_0 m_i}$ denotes the background Alfvén velocity. We remark that, having chosen the background magnetic field to be aligned with the z axis, the parallel component of the gradient coincides with ∂_z, whereas $\boldsymbol{\nabla}_\perp = \left(\partial_x, \partial_y\right)$, hence $\Delta_\perp = \partial_x^2 + \partial_y^2$. It is worth noting that the electric field dynamics are not affected by the electron and ion diamagnetic velocities which, for a constant magnetic field, turn out to be divergenceless.

In what follows, we assume a background pressure profile depending on the coordinate of x only and such that $dp_0/dx = -p_0/l_0$, where l_0 is a fixed spatial length. In other words, we consider an exponential behavior of the background pressure, which would require, for a precise force balance, an additional dependence of the magnetic field z-component of the form $4\pi p_0/B_0$, which will be neglected in what follows since, in a Tokamak, the plasma β-parameter is rather small. If we denote by $\bar{p}$ the pressure contrast (the fluctuation value to the background one, i.e., $\bar{p} = \frac{\delta p}{p_0}$), it obeys the following equation (the same for ions and electrons):

$$\partial_t \bar{p} + \frac{c}{B_0}\left(\partial_x \phi \partial_y \bar{p} - \partial_y \phi \partial_x \bar{p}\right) = -\frac{c}{B_0 l_0} \partial_y \phi + \partial_z \left(\frac{1}{n_0 e} j_z - u_z\right), \tag{6}$$

u_z is the ion parallel fluctuating velocity.The equation governing the dynamics of u_z reads

$$\partial_t u_z + \frac{c}{B_0}\left(\partial_x \phi \partial_y u_z - \partial_y \phi \partial_x u_z\right) = -\frac{2K_B T_0}{M_i} \partial_z \bar{p} \,. \tag{7}$$

where T_0 is the background temperature common to ions and electrons, linked to the background pressure via $p_0 = n_0 K_B T_0$, with K_B as the Boltzmann constant. If we denote the perturbation of the parallel magnetic vector potential as $\mathbf{A}_\parallel \equiv \psi \mathbf{e}_z$, then we easily get from the Ampere law (displacement currents are negligible in a non-relativistic plasma) the relation of

$$\mathbf{j}_\parallel = -\frac{c}{4\pi} \Delta_\perp \psi \, \mathbf{e}_z \,, \tag{8}$$

connecting the parallel current to the turbulent fluctuating magnetic field. The system describing the perturbation dynamics is completed by the generalized Ohm law, taking the explicit form of

$$\frac{1}{c} \partial_t \psi = \frac{c}{4\pi\sigma} \Delta_\perp \psi + \partial_z \left(\frac{K_B T_0}{e} \bar{p} - \phi\right), \tag{9}$$

where $\sigma \equiv 1.96\, n_0 e^2/m_e \nu_{ei}$ denotes the electric parallel conductivity, with m_e as the electron mass and ν_{ei} as the electron–ion collision frequency. We conclude the construction of this dynamical scenario by stressing the relations between the electric field components and the potentials, i.e., $\mathbf{E}_\perp = -\boldsymbol{\nabla}_\perp \phi$ and $E_z = -\partial_z \phi - \frac{1}{c}\partial_t \psi$.

We now aim to formulate the dynamical system, derived above, by means of dimensionless quantities. To this end, we introduce new space and time coordinates as $u \equiv x/L$, $v \equiv y/L$, $w \equiv (2\pi z)/R$ and $\tau \equiv \Omega_i t$. Here, L and R are two spatial scales (we assume $R \gg L$) characterizing the poloidal plane and the toroidal direction, respectively. Analogously, we define the new set of dynamical variables as $\Phi \equiv e\phi/K_B T$, $\Psi \equiv e\psi/K_B T$

and $U \equiv (2\pi u_z)/(\Omega_i R)$. The fourth unknown $\bar{p}$ is dimensionless by definition. We also introduce $D_\perp \equiv \partial_u^2 + \partial_v^2$.

In terms of this set of redefined coordinates and variables, Equations (5)–(7) and (9) take the explicit form:

$$\partial_\tau D_\perp \Phi + A\{\Phi, D_\perp \Phi\} = -BD_\perp \partial_w \Psi + CD_\perp^2 \Phi\,, \tag{10}$$

$$\partial_\tau \bar{p} + A\{\Phi, \bar{p}\} = -r_1 A \partial_v \Phi - \partial_w (DD_\perp \Psi + U)\,, \tag{11}$$

$$\partial_\tau U + A\{\Phi, U\} = -2r_2 A \partial_w \bar{p}\,, \tag{12}$$

$$\partial_\tau \Psi = ED_\perp \Psi + F\partial_w(\bar{p} - \Phi)\,, \tag{13}$$

where we introduced the dimensionless version of the constants characterizing the physical features of our model as

$$A \equiv \frac{K_B T_0}{M_i \Omega_i^2 L^2}\,, \quad B \equiv \frac{2\pi v_A^2}{c\Omega_i R}\,, \quad C \equiv \frac{\nu}{\Omega_i L^2}\,, \tag{14}$$

$$D \equiv \frac{2\pi c \lambda_D^2}{L^2 \Omega_i R}\,, \quad E \equiv \frac{c^2}{4\pi \Omega_i \sigma L^2}\,, \quad F \equiv \frac{2\pi c}{\Omega_i R}\,, \tag{15}$$

$$r_1 \equiv \frac{L}{l_0}\,, \quad r_2 \equiv \frac{4\pi^2 L^2}{R^2}. \tag{16}$$

The standard symbol λ_D indicates the Debye length, and we observe that $A \equiv \bar{\rho}_i^2$, being that $\bar{\rho}_i$ is the ion Larmor radius normalized with the poloidal length scale, i.e., $\bar{\rho}_i = \rho_i / L$.

Finally, we also adopted the compact notation of

$$\{\Phi, f\} \equiv \partial_u \Phi \partial_v f - \partial_v \Phi \partial_u f\,, \tag{17}$$

where f is a generic scalar function of the spatial coordinates (u, v). The system above corresponds to a closed set of partial differential equations in the four unknowns, Φ, $\bar{p}$, U and Ψ, which, once assigned suitable initial and boundary conditions (see below), provides a description of the plasma turbulent dynamics.

3. Generalized Hasegawa–Wakatani Model

In this section, we show that the set of dynamical equations derived above is equivalent to a generalized Hasegawa–Wakatani model. Indeed, by expressing the quantity $D_\perp \Psi$, i.e., the current density, from Equation (13) into Equations (10) and (11), we get the following two restated equations

$$\partial_\tau D_\perp \Phi + \rho_i^2 \{\Phi, D_\perp \Phi\} = -\iota \partial_\tau \partial_w \Psi + \eta \partial_w^2 (\bar{p} - \Phi) + CD_\perp^2 \Phi\,, \tag{18}$$

$$\partial_\tau \bar{p} + \rho_i^2 \{\Phi, \bar{p}\} = -r_1 \rho_i^2 \partial_v \Phi - \delta \partial_\tau \partial_w \Psi + \epsilon \partial_w^2 (\bar{p} - \Phi) - \partial_w U + \mathcal{D}_p D_\perp \bar{p}\,, \tag{19}$$

where we redefined the coupling constants of our model as

$$\iota \equiv \frac{B}{E}\,, \; \eta \equiv \frac{BF}{E}, \tag{20}$$

$$\delta \equiv \frac{D}{E}\,, \; \epsilon \equiv \frac{DF}{E}\,. \tag{21}$$

In Equation (19), we added a diffusion term ($\mathcal{D}_p$ being a constant diffusion coefficient) to account for different transport regimes in a Tokamak edge plasma.

It is worth noting that, in our scheme, the kinetic viscosity ν and the electron–ion collision frequency ν_{ie} are constants, independent of the spatial point and the instant of time considered. Hence, the parameters ι, η, δ and ϵ are mere positive real numbers and the set (12), (18) and (19) is a system of PDE with constant coefficients. The same does not hold for Equation (13): indeed, in this case, an explicit dependence on the specific point considered is present, due to the background density $n_0(x)$ appearing in the definition of

the parallel conductivity σ. In order to deal with a system of PDE with constant coefficients, one can approximate the number density $n_0(x) = n^* e^{-x/l_0}$ (n^* denoting the X-point number density) with its mean value on the interval $-l_0/2 \leq x \leq l_0/2$, resulting in $n_0 = 2n^* \sinh(1/2)$.

Now, as the fourth equation for the four unknowns, Φ, $\bar{p}$, U and Ψ, instead of Equation (13), we consider Equation (10), which we recast as

$$D_\perp(\partial_\tau \Phi + B\partial_w \Psi) = -\rho_i^2 \{\Phi\,,\, D_\perp \phi\} + C D_\perp^2 \Phi\,. \tag{22}$$

We observe that, in the linearized inviscid case, the equation above would correspond to the Lorentz gauge condition, as restricted to the present symmetry.

4. Relevant Reduced Model

We now focus our attention on a reduced model, described by a single equation for the electric potential. To this end, we neglect, in the system (18), (19) and (12), two quantities that are usually small in many turbulence configurations of a Tokamak, i.e., the gradient of the background pressure p_0 (responsible for a linear instability) and the presence of the velocity U in the problem. Hence, we take the limit $l_0 \to \infty$ in Equations (18) and (19) and we neglect Equation (12). From a physical point of view, taking the limit $l_0 \to \infty$, we are simply stating that the typical scale of the background pressure variation is much larger than the corresponding spatial scale of the turbulent dynamics. It is just in this situation that we can neglect the background pressure gradients in comparison to the fluctuating pressure fluctuations. Under these assumptions, Equation (19) is rewritten as

$$\partial_\tau \bar{p} + \rho_i^2 \{\Phi, \bar{p}\} = -\delta \partial_\tau \partial_w \Psi + \epsilon \partial_w^2 (\bar{p} - \Phi) + \mathcal{D}_p D_\perp \bar{p}\,. \tag{23}$$

If we now set $\mathcal{D}_p \equiv C$, we notice that Equations (18) and (23) result identicalyl, provided the constitutive relation of

$$D_\perp \Phi = \frac{B}{D} \bar{p} \tag{24}$$

to be implemented. Inserting (24) into the equation for the electric potential (18) yields

$$\partial_\tau D_\perp \Phi + \rho_i^2 \{\Phi\,, D_\perp \Phi\} = -\iota \partial_\tau \partial_w \Psi + \eta \partial_w^2 (q D_\perp \Phi - \Phi) + C D_\perp^2 \Phi\,, \tag{25}$$

with $q \equiv D/B$. In this way we reduced the dynamical system composed by Equations (12), (18), (19) and (22) to a set of two coupled Equations (22) and (25), equipped with the supplemental constitutive relation (24). Now, if we apply to Equation (25) the operator $D_\perp$ and we make use of Equation (22), we obtain a single equation characterizing our model, in which the only unknown is the electric potential, namely

$$\begin{aligned} \partial_\tau \big(D_\perp - \tfrac{\iota}{B}\partial_\tau\big) D_\perp \Phi + \rho_i^2 \big(D_\perp - \tfrac{\iota}{B}\partial_\tau\big)\{\Phi\,, D_\perp \Phi\} \\ = \eta \partial_w^2 D_\perp (q D_\perp \Phi - \Phi) + C\big(D_\perp - \tfrac{\iota}{B}\partial_\tau\big) D_\perp^2 \Phi\,. \end{aligned} \tag{26}$$

We remark that the terms times ι/B vanish for the axisymmetric component of the theory, due to the fact that they represent derivatives along the toroidal direction of the vector potential.

We are now interested in analyzing the properties of Equation (26). To this end, we exploit the periodicity of the system on the coordinate w and we express the electric potential through a Fourier series along the toroidal direction. The poloidal plane coordinates (u, v) will be treated instead with a Fourier transform, in order to obtain

$$\Phi(\tau, u, v, w) = \sum_{n=-\infty}^{\infty} \int_D \frac{dk_u dk_v}{(2\pi)^2}\, \zeta_{\mathbf{k}}^n\, e^{i(k_u u + k_v v + nw)}\,, \tag{27}$$

where $\xi^n_{\mathbf{k}} = \xi^n(\tau, k_u, k_v)$. The region D is an annulus of major radius $k_{max} = 2\pi/\rho_i$, corresponding to the cut-off value of the drift-fluid approximation here addressed. The local character of our analysis also implies a lower-bound k_{min} for the poloidal wavenumber, connected to the size of the region in which the assumptions we made, for instance, a purely toroidal magnetic field, result validly.

Substituting into Equation (26), we get the following basic equation for the Fourier modes

$$\begin{aligned} k^2\left(k^2 + p\partial_\tau\right)\partial_\tau\xi^n_{\mathbf{k}} + \rho_i^2\left(k^2 + p\partial_\tau\right)\sum_{m=-\infty}^{\infty}\int \tfrac{dq_u dq_v}{(2\pi)^2} q^2(k_u q_v - k_v q_u)\xi^{n-m}_{\mathbf{k}-\mathbf{q}}\xi^m_{\mathbf{q}} \\ = -\eta n^2 k^2\left(qk^2+1\right)\xi^n_{\mathbf{k}} - Ck^4\left(k^2 + p\partial_\tau\right)\xi^n_{\mathbf{k}}\,, \end{aligned} \tag{28}$$

where $p \equiv \iota/B$ and $k = \sqrt{k_u^2 + k_v^2}$ is the norm of the poloidal wavenumber. It is easy to verify that the $n = 0$ mode satisfies

$$k^2\partial_\tau\xi^0_{\mathbf{k}} + \rho_i^2\int_D \frac{dq_u dq_v}{(2\pi)^3} q^2(k_u q_v - k_v q_u)\xi^0_{\mathbf{k}-\mathbf{q}}\xi^0_{\mathbf{q}} + Ck^4\xi^0_{\mathbf{k}} = 0\,. \tag{29}$$

In the inviscid limit ($C \equiv 0$), the equation above is characterized by a statistical equilibrium [21,25], corresponding to an energy spectrum of the form

$$E(k) = \frac{1}{\alpha + \beta k^2}\,, \tag{30}$$

where the parameters α and β represent two inverse temperatures, associated with the energy and enstrophy constants of motion, respectively.

As in [21], we now concentrate our attention on the case in which α can be neglected in the energy spectrum (30) (this choice is linked to a specific structure of the system initialization), for which we deal with a constant enstrophy isotropic spectrum. The corresponding mode amplitude results in

$$\xi^0_k = \frac{\Gamma}{k^2}\,, \tag{31}$$

where Γ is a complex constant. It is easy to verify that the field form (31) is a steady solution of Equation (29) in the inviscid case $C \equiv 0$ (for details, see Appendix A). Clearly, it remains a good approximate solution also for the viscous case, when $Ck^2 \mid \Gamma \mid \ll 1$, and this regime remains valid for a significant part of the inertial region spectrum. It is worth noting that the steady spectrum above is a mean value of the field Fourier strength, around which the fluctuations evolve. From a practical point of view, this can be determined via a numerical analysis of the Fourier dynamic representation, by looking at a well-developed turbulence regime and averaging the field fluctuations on a given time interval (ideally the smallest possible) over which the emerging average is really steady; see the studies in [20–22].

We now linearize Equation (28) in the generic $n \neq 0$ mode, when considering the steady solution (31) as the dominant contribution, namely,

$$\begin{aligned} k^2\left(k^2 + p\partial_\tau\right)\partial_\tau\xi^n_{\mathbf{k}} + \rho_i^2\left(k^2 + p\partial_\tau\right)\int \tfrac{dq_u dq_v}{(2\pi)^2} q^2(k_u q_v - k_v q_u)\left[\xi^n_{\mathbf{k}-\mathbf{q}}\xi^0_{\mathbf{q}} + \xi^0_{\mathbf{k}-\mathbf{q}}\xi^n_{\mathbf{q}}\right] = \\ - \eta n^2 k^2\left(qk^2+1\right)\xi^n_{\mathbf{k}} - Ck^4\left(k^2 + p\partial_\tau\right)\xi^n_{\mathbf{k}}\,. \end{aligned} \tag{32}$$

By assuming isotropy in the poloidal plane, i.e., $\xi^n_{\mathbf{k}} = f^n(k,\tau)$, we see that the term containing the integral identically vanishes (details in Appendix A) and the dynamical equation for the Fourier modes f^n results in

$$\left(k^2 + p\partial_\tau\right)\partial_\tau f^n = -\eta n^2\left(qk^2+1\right)f^n - Ck^2\left(k^2 + p\partial_\tau\right)f^n\,. \tag{33}$$

We are interested in analyzing the dispersion relation and the damping rate for these modes; hence, we search for a solution to the above equation in the form of $f^n = \bar{f}^n \exp\{-i\Omega(k)\tau\}$ (with $\bar{f}^n$ being a constant and Ω a complex number), obtaining

$$p\Omega^2 + (1+Cp)k^2 i\Omega - \eta n^2(qk^2+1) - Ck^4 = 0\,. \tag{34}$$

We explicitly denote the real and imaginary part of Ω as ω and γ, respectively, i.e., $\Omega = \omega + i\gamma$ (with ω and γ being real functions of k). Then, Equation (34) splits into the following system

$$\begin{cases} p\left(\omega^2 - \gamma^2\right) - (1+Cp)k^2\gamma - \eta n^2\left(qk^2+1\right) - Ck^4 = 0 & (35) \\ \omega\left(2p\gamma + (1+Cp)k^2\right) = 0. & (36) \end{cases}$$

It is immediately noticeable that (36) is satisfied either for $\omega = 0$ or $\gamma = -\frac{1+Cp}{2p}k^2$. Inserting the $\omega = 0$ solution in (35) yields

$$\gamma_\pm = -\frac{1+Cp}{2p}k^2 \pm \frac{1}{2p}\sqrt{(1-Cp)^2k^4 - 4\eta p n^2(qk^2+1)}, \tag{37}$$

where the symbol $\pm$ identifies two distinct solutions, corresponding to the choice of either the plus or the minus sign in the right-handed side of the above equation. The solution denoted by a plus (minus) corresponds to a slow (fast) damping rate and the separation between the two regimes is depicted by the orange and green curves in Figure 1. The reality of both $\gamma_\pm$ is ensured by

$$k \geq \bar{k}_n = \sqrt{\frac{2\eta n^2 pq}{(1-Cp)^2}\left(1 + \sqrt{1 + \frac{(1-Cp)^2}{\eta n^2 pq^2}}\right)}. \tag{38}$$

We remark that, when (38) is satisfied, both $\gamma_\pm$ are real negative numbers and the corresponding solution describes damped oscillations rather than wave-like fluctuations.

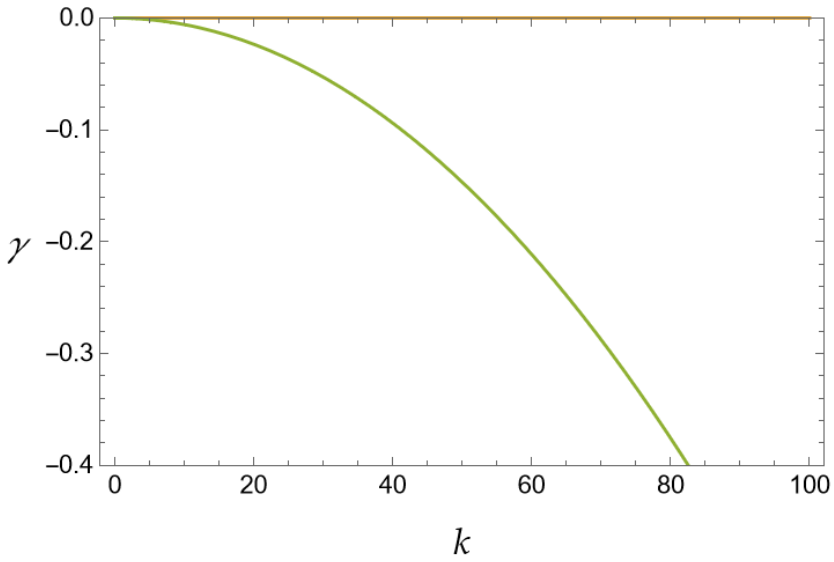

Figure 1. *Cont.*

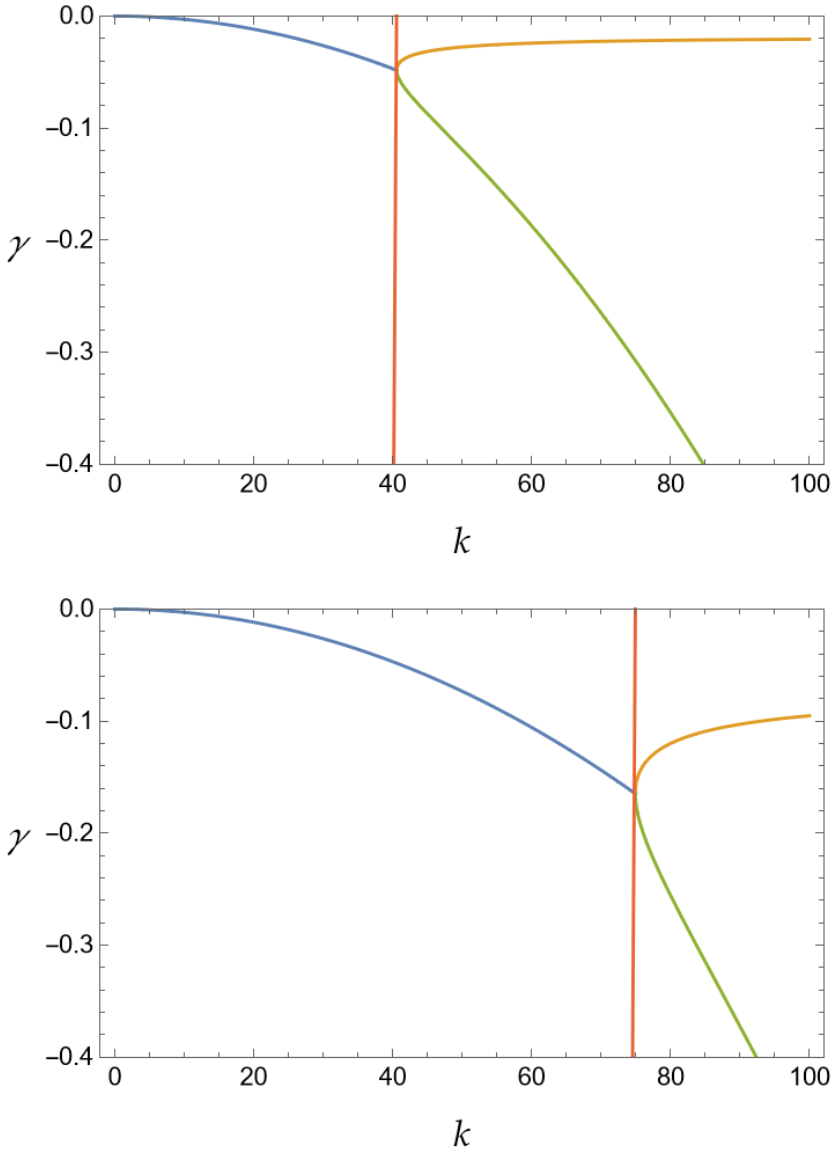

Figure 1. Damping coefficients for values of the toroidal wavenumber $n = 0, 1, 2$ (top to bottom): the blue curve is relative to the wave-like regime ($\omega \neq 0$), whereas the orange and green curves represent γ_+ and γ_-, respectively, characterizing the pure damping regime ($\omega = 0$). The red vertical line indicates the value of the characteristic wavenumber $\bar{k}_n$ separating the two regimes. We plot the norm of the poloidal wavenumber k on the horizontal axis and the value of the damping coefficient on the vertical one.

Conversely, by selecting the second solution of (36), i.e., $\gamma = -\frac{1+Cp}{2p}k^2$, and solving (35) for the angular frequency ω, we obtain

$$\omega_\pm = \pm\frac{1}{2p}\sqrt{-(1-Cp)^2k^4 + 4\eta p n^2(qk^2+1)}, \tag{39}$$

and in this case, the reality condition on $\omega_\pm$ is satisfied for $k < \bar{k}_n$. It is interesting to compute the group velocity for these wave-like solutions, which reads

$$v_g = \mp\frac{k}{p}\frac{(1-Cp)^2k^2 - 2\eta n^2 pq}{\sqrt{-(1-Cp)^2k^4 + 4\eta p n^2(qk^2+1)}}. \tag{40}$$

We outline that the group velocity has the opposite sign with respect to the phase velocity $v_p = \frac{\omega}{k}$ when

$$k > k_n^0 = \sqrt{\frac{2\eta n^2 pq}{(1 - Cp)^2}}, \tag{41}$$

whereas both velocities share the same sign in the opposite case $k < k_n^0$. Lastly, for $k = k_n^0$, we deal with a wave-like solution characterized by a null group velocity, i.e., no energy transport is allowed in this regime. It must be stressed that k_n^0 is always smaller than $\bar{k}_n$; therefore, for any given $n > 0$, one can always select a wavenumber k such that the wave-like solutions associated with $\omega_\pm$ have concordant, discordant or null group velocity. In order to provide some quantitative examples of the phenomenology here described, let us assume typical values of a Tokamak-like environment [19,23,24] for the physical parameters characterizing our model: specifically, we set $T = 100$ eV, $B_0 = 3$ T and $n_0 = 5 \times 10^{19}$ m^{-3} [23]; thus, $\Omega_i \simeq 1.4 \times 10^8$ s^{-1} and $\rho_i \simeq 0.048$ cm. Moreover, we select for the length scales L and R values equal to 1 cm and 1300 cm, respectively. We report, in Figure 2, the different regimes for the solutions of (34) described above, highlighting the fact that either a pure damped oscillatory fluctuation or wave-like decaying propagating ripples are present, depending on the specific choice of the toroidal an poloidal wavenumbers considered. For instance, the axisymmetric $n = 0$ solution admits solely a pure damped oscillatory regime; for $1 \leq n \leq 3$, all three regimes (either oscillatory or wave-like with concordant or discordant velocities) are feasible and the specific configuration depends on the poloidal wavenumber k; for n equal to 4 and 5, only the wave-like solutions are allowed, whereas for $n > 5$, the system has a unique solution, corresponding to the wave-like case with concordant velocities.

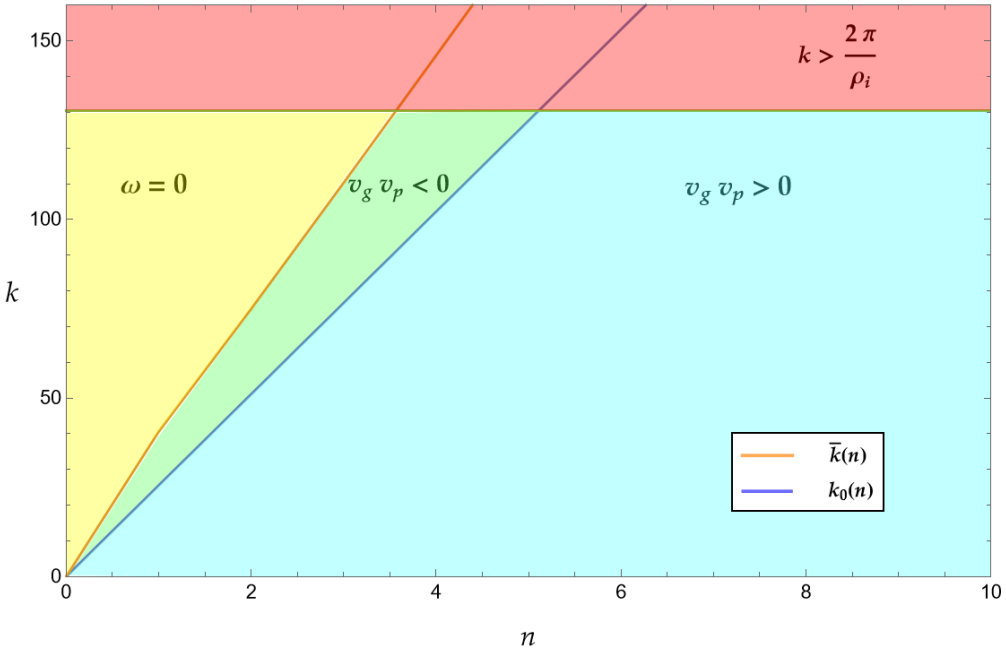

Figure 2. Different regimes for the solution of (34): the area in yellow indicates the solution with $\omega = 0$, the sectors in green and light blue represent wave-like solutions having group and phase velocities that are discordant or concordant, respectively. The orange and blue lines depict the characteristic wavenumbers $\bar{k}_n$ and k_n^0 as functions of the toroidal wavenumber n, with the latter ranging on the horizontal axis. On the vertical axis, we plot the norm of the poloidal wavenumber $k = \sqrt{k_u^2 + k_v^2}$. The region in red represents values of k greater than the cut-off $2\pi/\rho_i$, for which the fluid description adopted in this work cannot be enforced.

In Figure 1 we show the behavior of the damping coefficients as functions of the poloidal wavenumber k, outlining again the transition between wave-like and oscillatory regimes marked by the threshold wavenumber $\bar{k}_n$. We can observe that, for growing values of n, the latter moves towards larger values of k.

5. Concluding Remarks

We developed a low-frequency formulation for the two-fluid turbulence in the edge region of a Tokamak plasma, whose magnetic configuration was associated with a constant and uniform axial magnetic field, i.e., well-representing a region very close to the X-point [26].

Then, under suitable assumptions, based on the standard operational regimes of medium-size and incoming experiments, we reduced the dynamics to a simplified model: actually, we deal with a single equation for the electric potential field, a constitutive relation giving the pressure fluctuations and an evolutionary link between the scalar (electric) and vector (de facto the axial component) potentials.

In order to better focus on the physical characteristics of these assumptions, we recall that they can be summarized in the following three statements: (i) the background pressure gradients are negligible; (ii) the ion axial velocity can be neglected with respect to the corresponding contribution for electrons; and (iii) the shear viscosity and particle diffusion coefficients are taken to be comparable. The first assumption is justified by the fact that the background pressure gradient, in a realistic Tokamak configuration, is naturally suppressed by means of magnetic shear [9]. The second hypothesis provides a good representation of the Tokamak typical plasmas in the absence of spontaneous rotation [27] or of neutral beam injection. Finally, the possibility to take the viscosity and diffusivity coefficients of the same order has been considered in various formulations, see, for instance, [18], and this is due to the role that the higher-order Laplacian operators take in the edge turbulence picture. In fact, the value of these coefficients is relevant in stabilizing the numerical simulation and, de facto, their amplitude cannot be predicted *a priori*, simply because it is directly and significantly influenced by the turbulence features. Thus, the value of the dissipation coefficients has a natural phenomenological impact and different regimes can be investigated.

The main result of the present analysis is to recognize that, also in the presence of a fluctuating poloidal magnetic field, the 3D-turbulence picture, i.e., in which non-axially symmetric modes are present, has a natural branch of the non-linear dynamics along which it decays toward a two-dimensional profile. This result generalizes the study in [20], concerning the electrostatic turbulence only. Although the attractive nature of the axially symmetric turbulence emerges in both cases, here, we found a different morphology of the decaying rate: while in the electrostatic scenario, the growth rate depends on n^2 and a single branch is present, here, this same quantity is associated with dissipation coefficients, but, below a given wavenumber, it is independent of the toroidal index n. Furthermore, a second branch emerged for wavenumbers above the threshold provided by the parameter $\bar{k}_n$ introduced in this work, and in this case, a dependence on the axial number n is restored. However, it is important to remark that no peculiar limit exists to recover the pure electrostatic case from the electromagnetic analysis. It is merely this fact that clarifies the relevance of dealing with a fluctuating poloidal magnetic field, since it is able to induce, especially for high values of the β-parameter of the plasma, a specific fingerprint on the turbulent dynamics as a whole. The present theoretical construction could be validated by a numerical investigation of the considered non-linear dynamics. The comparison of the general picture discussed in Section 2, with the reduced model proposed in Section 4, could make the quantitative conditions under which our model becomes fully predictive more precise, and this perspective could be the subject of a natural follow-up to this study. Anyway, for what concerns the decaying behavior of the 3D turbulence towards a 2D axially symmetric scenario, we can be confident that the situation is very similar to the investigation performed in [20] on the electrostatic turbulence. In other

words, in correspondence with that result (which is contained in the present scenario), we are lead to argue that the decaying branch we identified here has a rather general character. Also, in the electromagnetic turbulence, the axially symmetric fluctuations significantly attract the nonlinear 3D dynamics and the mode correspondent to $n = 0$ turns out to be the most energetic one.

Author Contributions: Conceptualization, G.M.; Investigation, G.M. and F.M.; Writing– review and editing, G.M. and F.M. All authors have read and agreed to the published version of the manuscript.

Funding: This research received no external funding.

Data Availability Statement: Data is contained within the article.

Acknowledgments: We would like to thank Francesco Cianfrani for the interesting and useful discussions on the possible implementation of a gauge condition in the considered dynamics.

Conflicts of Interest: The authors declare no conflicts of interest.

Appendix A

Here, we show that the terms containing integrals in Equations (29) and (32) vanish under the assumptions $\zeta_k^0 = \frac{\Gamma}{k^2}$ and $\zeta_{\mathbf{k}}^n = f_k^n$. To begin, let us focus on the $n = 0$ case, which we report here, for the sake of clarity,

$$\int_D dq_u dq_v \, q^2 (k_u q_v - k_v q_u) \frac{\Gamma}{|\mathbf{k} - \mathbf{q}|^2} \frac{\Gamma}{q^2}.$$

We express both the vectors $\mathbf{q}$ and $\mathbf{k}$ in polar coordinates, i.e.,

$$\begin{aligned} q_u &= r \cos\theta & k_u &= \rho \cos\varphi \\ q_v &= r \sin\theta & k_v &= \rho \sin\varphi \end{aligned}$$

where ρ and φ are two constants. The integral rewrites

$$\int_{k_{min}}^{k_{max}} dr \, r^4 \int_0^{2\pi} d\theta \, \sin(\theta - \varphi) \left[\frac{1}{r^2} + \frac{1}{r^2 + \rho^2 - 2\rho r \cos(\theta - \varphi)} \right],$$

where we discarded constant factors. By exploiting the periodicity of the trigonometric functions, it is immediately verifiable that the expression above is identically null. We now turn our attention to the $n \neq 0$ case, in which the integral has the form of

$$\int_D dq_u dq_v q^2 (k_u q_v - k_v q_u) \left[f^n_{|\mathbf{k}-\mathbf{q}|} \frac{\Gamma}{q^2} + \frac{\Gamma}{|\mathbf{k} - \mathbf{q}|^2} f_q^n \right].$$

By resorting, as before, to polar coordinates and expanding the Fourier mode f_q^n in Taylor series, i.e.,

$$f_q^n = \sum_{m=0}^{\infty} c_m^n \, q^m = \sum_{m=0}^{\infty} c_m^n \, r^m,$$

with c_m^n a matrix of real coefficients, we observe that the integral reads as

$$\int_{k_{min}}^{k_{max}} dr \, r^4 \int_0^{2\pi} d\theta \, \sin(\theta - \varphi) \left[\frac{\left(r^2 + \rho^2 - 2\rho r \cos(\theta - \varphi)\right)^{\frac{m}{2}}}{r^2} + \frac{r^m}{r^2 + \rho^2 - 2\rho r \cos(\theta - \varphi)} \right],$$

where m is an integer non-negative number. Again, it sufficient to invoke the periodicity of the trigonometric functions to demonstrate that, also in this case, the integral turns out to be identically null.

References

1. Wesson, J.; Campbell, D. *Tokamaks*; International Series of Monographs on Physics; OUP: Oxford, UK, 2011.
2. Tamain, P.; Bufferand, H.; Ciraolo, G.; Colin, C.; Galassi, D.; Ghendrih, P.; Schwander, F.; Serre, E. The TOKAM3X code for edge turbulence fluid simulations of tokamak plasmas in versatile magnetic geometries. *J. Comput. Phys.* **2016**, *321*, 606–623. [CrossRef]
3. Stegmeir, A.; Ross, A.; Body, T.; Francisquez, M.; Zholobenko, W.; Coster, D.; Maj, O.; Manz, P.; Jenko, F.; Rogers, B.; et al. Global turbulence simulations of the tokamak edge region with GRILLIX. *Phys. Plasmas* **2019**, *26*, 052517. [CrossRef]
4. Cianfrani, F.; Fuhr, G.; Beyer, P. Edge plasma relaxations due to diamagnetic stabilization. *Phys. Plasmas* **2022**, *29*, 032302. [CrossRef]
5. Oliveira, D.; Body, T.; Galassi, D.; Theiler, C.; Laribi, E.; Tamain, P.; Stegmeir, A.; Giacomin, M.; Zholobenko, W.; Ricci, P.; et al. Validation of edge turbulence codes against the TCV-X21 diverted L-mode reference case. *Nucl. Fusion* **2022**, *62*, 096001. [CrossRef]
6. Graves, J.P.; Horacek, J.; Pitts, R.A.; Hopcraft, K.I. Self-similar density turbulence in the TCV tokamak scrape-off layer. *Plasma Phys. Control. Fusion* **2005**, *47*, L1. [CrossRef]
7. Zweben, S.J.; Boedo, J.A.; Grulke, O.; Hidalgo, C.; LaBombard, B.; Maqueda, R.J.; Scarin, P.; Terry, J.L. Edge turbulence measurements in toroidal fusion devices. *Plasma Phys. Control. Fusion* **2007**, *49*, S1. [CrossRef]
8. Scott, B. The nonlinear drift wave instability and its role in tokamak edge turbulence. *New J. Phys.* **2002**, *52*, 352. [CrossRef]
9. Scott, B.D. Tokamak edge turbulence: Background theory and computation. *Plasma Phys. Control. Fusion* **2007**, *49*, S25. [CrossRef]
10. Hasegawa, A.; Wakatani, M. Plasma Edge Turbulence. *Phys. Rev. Lett.* **1983**, *50*, 682–686. [CrossRef]
11. Hasegawa, A.; Wakatani, M. Self-Organization of Electrostatic Turbulence in a Cylindrical Plasma. *Phys. Rev. Lett.* **1987**, *57*, 1581–1584. [CrossRef]
12. Hasegawa, A.; Mima, K. Strong turbulence, self-organization and plasma confinement. *Eur. Phys. J. H* **2018**, *43*, 499–521. [CrossRef]
13. Diamond, P.H.; Hasegawa, A.; Mima, K. Vorticity dynamics, drift wave turbulence, and zonal flows: A look back and a look ahead. *Plasma Phys. Control. Fusion* **2011**, *53*, 124001. [CrossRef]
14. Kraichnan, R.H.; Montgomery, D. Two-dimensional turbulence. *Rep. Prog. Phys.* **1980**, *43*, 547. [CrossRef]
15. Boffetta, G.; Ecke, R.E. Two-Dimensional Turbulence. *Annu. Rev. Fluid Mech.* **2012**, *44*, 427–451. [CrossRef]
16. Kraichnan, R.H. Inertial Ranges in Two-Dimensional Turbulence. *Phys. Fluids* **1967**, *10*, 1417–1423. [CrossRef]
17. Kraichnan, R.H. Statistical dynamics of two-dimensional flow. *J. Fluid Mech.* **1975**, *67*, 155–175. [CrossRef]
18. Biskamp, D.; Zeiler, A. Nonlinear Instability Mechanism in 3D Collisional Drift-Wave Turbulence. *Phys. Rev. Lett.* **1995**, *74*, 706–709. [CrossRef]
19. Cianfrani, F.; Montani, G. On the edge turbulence in a DTT-like tokamak plasma. *arXiv* **2024**, arXiv:2405.09837. [CrossRef].
20. Montani, G.; Carlevaro, N. On the 3D turbulence regime in a Tokamak plasma edge. *Phys. D Nonlinear Phenom.* **2023**, *451*, 133774. [CrossRef]
21. Montani, G.; Carlevaro, N.; Tirozzi, B. On the Turbulent Behavior of a Magnetically Confined Plasma near the X-Point. *Fluids* **2022**, *7*, 157. [CrossRef]
22. Carlevaro, N.; Montani, G.; Moretti, F. On the Effects of Tokamak Plasma Edge Symmetries on Turbulence Relaxation. *Symmetry* **2023**, *15*, 1745. [CrossRef]
23. Albanese, R.; Crisanti, F.; Martin, P.; Pizzuto, A.; Mazzitelli, G.; Tuccillo, A.; Ambrosino, R.; Appi, A.; Di Gironimo, G.; Di Zenobio, A.; et al. Design review for the Italian Divertor Tokamak Test facility. *Fus. Eng. Des.* **2019**, *146*, 194–197. [CrossRef]
24. Ambrosino, R. DTT—Divertor Tokamak Test facility: A testbed for DEMO. *Fus. Eng. Des.* **2021**, *167*, 112330. [CrossRef]
25. Seyler, C.; Salu, Y.; Montgomery, D.; Knorr, G. Two-dimensional turbulence in inviscid fluids or guiding center plasmas. *Phys. Fluids* **1975**, *18*, 803–813. [CrossRef]
26. Ryutov, D.D.; Soukhanovskii, V.A. The snowflake divertor. *Phys. Plasmas* **2015**, *22*, 110901. [CrossRef]
27. Sonnino, G.; Cardinali, A.; Sonnino, A.; Nardone, P.; Steinbrecher, G.; Zonca, F. A note on the application of the Prigogine theorem to rotation of tokamak-plasmas in absence of external torques. *Chaos Interdiscip. J. Nonlinear Sci.* **2014**, *24*, 013129. [CrossRef]

Disclaimer/Publisher's Note: The statements, opinions and data contained in all publications are solely those of the individual author(s) and contributor(s) and not of MDPI and/or the editor(s). MDPI and/or the editor(s) disclaim responsibility for any injury to people or property resulting from any ideas, methods, instructions or products referred to in the content.